

Phase transitions and Bose-Einstein condensation in alpha-nucleon matter

L. M. Satarov,^{1,2} I. N. Mishustin,^{1,2} A. Motornenko,^{1,3}
V. Vovchenko,^{1,3} M. I. Gorenstein,^{1,4} and H. Stoecker^{1,3,5}

¹ *Frankfurt Institute for Advanced Studies,
D-60438 Frankfurt am Main, Germany*

² *National Research Center "Kurchatov Institute" 123182 Moscow, Russia*

³ *Institut für Theoretische Physik, Goethe Universität Frankfurt,
D-60438 Frankfurt am Main, Germany*

⁴ *Bogolyubov Institute for Theoretical Physics, 03680 Kiev, Ukraine*

⁵ *GSI Helmholtzzentrum für Schwerionenforschung GmbH, D-64291 Darmstadt, Germany*

Abstract

The equation of state and phase diagram of isospin-symmetric chemically equilibrated mixture of alpha particles α and nucleons N are studied in the mean-field approximation. The model takes into account the effects of Fermi and Bose statistics for N and α , respectively. We use Skyrme-like parametrization of the mean-field potentials as functions of partial densities n_α and n_N , which contain both attractive and repulsive terms. Parameters of these potentials are chosen by fitting known properties of pure N - and pure α -matter at zero temperature. The sensitivity of results to the choice of the αN attraction strength is investigated. The phase diagram of the $\alpha - N$ mixture is studied with a special attention paid to the liquid-gas phase transitions and the Bose-Einstein condensation of α particles. We have found two first-order phase transitions, stable and metastable, which differ significantly by the fractions of alpha particles. It is shown that states with alpha condensate are metastable.

I. INTRODUCTION

At subsaturation densities and low temperatures nuclear matter has a tendency for clusterization, when small and big nucleon clusters are formed under conditions of thermal and chemical equilibrium. This state of excited nuclear matter is realized in nuclear reactions at intermediate energies known as multi-fragmentation of nuclei [1]. It is believed that clusterized nuclear matter is also formed in outer regions of neutron-stars and in supernova explosions [2]. It may play an important role by providing "seed" nuclei for later nucleosynthesis.

Different models have been used to describe the clusterized nuclear matter. In particular, the statistical approach turned out to be very successful to explain the mass and energy distributions of fragments and hadrons produced in heavy-ion collisions, see e.g. Refs. [3, 4]. Another powerful method is to perform molecular-dynamical simulations in a box taking into account effective interactions between nucleons, as it was done, e.g., in Ref. [5].

To better understand properties of clusterized nuclear matter one should use more realistic interactions between different clusters and take into account phenomenological constraints. In our recent paper [6] we studied the equation of state (EoS) of an idealized system composed entirely of α -particles. Their interaction was described by a Skyrme-like mean-field potential. We have found that such a system exhibits two interesting phenomena, namely, the Bose-Einstein condensation (BEC) and the liquid-gas phase transition (LGPT). Earlier the cold alpha matter has been considered microscopically by using phenomenological $\alpha\alpha$ potentials in Refs. [7–9], the lattice calculations were made in Ref. [10] and the relativistic mean-field (RMF) approach was applied in Ref. [11]. Properties of cold α chains have been discussed in Refs. [12–14].

However, by introducing such one-component system one disregards a possible dissociation of alphas into lighter clusters and nucleons. This process should be important at nonzero temperatures and large enough baryon densities. Binary $\alpha - N$ matter in chemical equilibrium with respect to reactions $\alpha \leftrightarrow 4N$ has been considered in [15] by using the virial approach. One should have in mind that the results of Ref. [15] may be justified only at small baryon densities. The two-component van der Waals model with excluded-volume repulsion has been developed to describe properties of $\alpha - N$ mixture in Ref. [16]. Note that both these approaches disregard possible BEC phenomena.

The EOS of matter composed of nucleons and nuclear clusters have been considered within different approaches including the liquid-drop model [2], several versions of the statistical model [17–19] and the RMF models [20–22]. In particular, in Ref. [21] the RMF calculations have been performed with the medium-dependent binding energy of alphas. Comparison of the excluded-volume and virial EoSs has been made in Ref. [23]. However, all these models do not include a possibility of BEC. This phenomenon was considered within the quasiparticle approach of Ref. [24], but only for dilute (nearly ideal-gas) mixtures of nucleons and nuclear clusters.

In the present paper we consider the isospin-symmetric $\alpha - N$ matter under the conditions of chemical equilibrium. The EoS of such matter is calculated in the mean-field approach using Skyrme-like parametrizations of the mean-field potentials. In this study we simultaneously take into account the LGPT and BEC effects.

The article is organized as follows. In Sec. II A we formulate main features of the model. The limit of ideal $\alpha - N$ gas is considered in Sec. II B and Appendix A. Pure nucleon and pure alpha matter with Skyrme interactions are studied in Sec. II C and II D, respectively. The results of these sections are used in choosing parameters of mean fields for $\alpha - N$ matter in Sec. III. The EoS and phase transitions of such matter are studied numerically in Sec. IV. Finally, the conclusions and outlook are given in Sec. V.

II. GENERAL REMARKS AND LIMITING CASES

A. Chemical equilibrium conditions

Let us consider the iso-symmetric system (with equal numbers of protons and neutrons) composed of nucleons N and alpha-particles α . A small difference between the proton and neutron masses and the Coulomb interaction effects will be neglected. Our consideration will be restricted to small temperatures $T \lesssim 30$ MeV. In this case, production of pions and other mesons, as well as excitation of baryonic resonances, like Δ and N^* , become negligible. Besides, the masses $m_N \simeq 938.9$ MeV and $m_\alpha \simeq 3727.3$ MeV are much larger than the system temperature, thus, a non-relativistic approximation can be used in the lowest order in T/m_N .

In the grand canonical ensemble the pressure $p(T, \mu)$ is a function of temperature T and baryon chemical potential μ . The latter is responsible for conservation of the baryon charge.

The chemical potential of N and α satisfy the relations

$$\mu_N = \mu, \quad \mu_\alpha = 4\mu, \quad (1)$$

which correspond to the condition of chemical equilibrium in the $N - \alpha$ mixture due to reactions $\alpha \leftrightarrow 4N$. The baryonic number density $n_B(T, \mu) = n_N + 4n_\alpha$, the entropy density $s(T, \mu)$, and the energy density $\varepsilon(T, \mu)$ can be calculated from $p(T, \mu)$ as

$$n_B = \left(\frac{\partial p}{\partial \mu} \right)_T, \quad s = \left(\frac{\partial p}{\partial T} \right)_\mu, \quad \varepsilon = Ts + \mu n_B - p \quad (2)$$

in the thermodynamic limit, where the system volume goes to infinity.

B. Ideal gas limit

Let us first consider the $\alpha - N$ system as a mixture of the ideal Fermi-gas of nucleons and the ideal Bose-gas of alpha. The pressure of such a system is equal to the sum of partial pressures

$$p^{\text{id}}(T, \mu) = p_N^{\text{id}}(T, \mu_N) + p_\alpha^{\text{id}}(T, \mu_\alpha). \quad (3)$$

Here ($\hbar = c = k_B = 1$):

$$p_i^{\text{id}}(T, \mu_i) = \frac{g_i}{(2\pi)^3} \int d^3k \frac{k^2}{3E_i} \left[\exp\left(\frac{E_i - \mu_i}{T}\right) \pm 1 \right]^{-1} \quad (i = N, \alpha), \quad (4)$$

where $E_i = \sqrt{m_i^2 + k^2}$ and g_i is the spin-isospin degeneracy factor ($g_\alpha = 1, g_N = 4$). Upper and lower signs in Eq. (4) correspond to $i = N$ and $i = \alpha$, respectively.

By taking derivatives with respect to μ_i one gets the partial densities

$$n_i = \left(\frac{\partial p_i^{\text{id}}}{\partial \mu_i} \right)_T = \frac{g_i}{(2\pi)^3} \int d^3k \left[\exp\left(\frac{E_i - \mu_i}{T}\right) \pm 1 \right]^{-1} \quad (i = N, \alpha). \quad (5)$$

In the following we will also use the canonical variables T, n_i as independent quantities. The transition from the grand canonical variables T, μ_i is made by solving the transcendental equations (5) with respect to μ_i . Allowable states of chemically equilibrated $\alpha - N$ mixture is then found using Eq. (1).

The chemical potential of α particles is restricted by the relation $\mu_\alpha \leq m_\alpha$. At $\mu_\alpha = m_\alpha$ the Bose condensation of α 's occurs. In this case a nonzero density of Bose-condensed (zero-momentum) alpha particles, n_{bc} , should be taken into account. By taking the lowest order

approximation in T/m_i (see Appendix) and introducing the thermal wave length of i th particle, $\lambda_i(T) = (2\pi/m_i T)^{1/2}$, one gets the following relations for the total density and pressure of α 's in the region of BEC:

$$n_\alpha = n_\alpha^*(T) + n_{bc}, \quad p_\alpha^{\text{id}} = p_\alpha^*(T) \quad (\mu_\alpha = m_\alpha). \quad (6)$$

Here

$$n_\alpha^*(T) = n_\alpha(T, \mu_\alpha \rightarrow m_\alpha - 0) \simeq \frac{g_\alpha}{\lambda_\alpha^3(T)} \zeta(3/2), \quad p_\alpha^*(T) \simeq \frac{g_\alpha T}{\lambda_\alpha^3(T)} \zeta(5/2), \quad (7)$$

where $\zeta(x) = \sum_{k=1}^{\infty} k^{-x}$ is the Riemann zeta function ($\zeta(3/2) \simeq 2.612$, $\zeta(5/2) \simeq 1.341$).

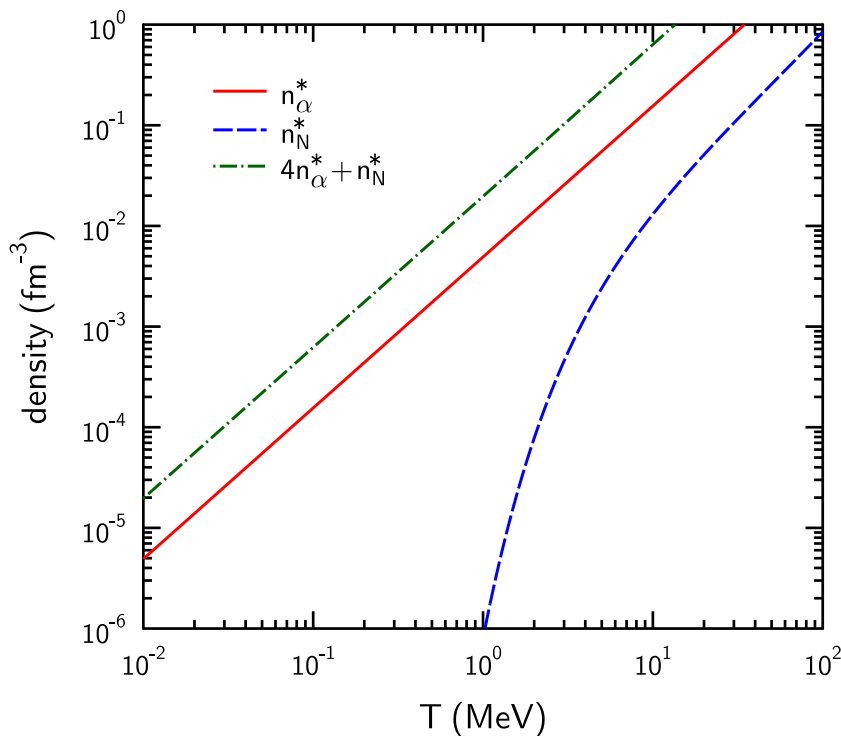


FIG. 1: Densities of alphas (the solid line), nucleons (the dashed curve), and the baryon density (the dash-dotted line) at BEC boundary as functions of temperature for ideal $\alpha - N$ gas.

The condition (1) leads to the relations $\mu \equiv \mu_N = \mu_\alpha/4 \leq m_\alpha/4 = m_N - B_\alpha$, where $B_\alpha = m_N - m_\alpha/4 \simeq 7.1$ MeV is the binding energy per baryon of the α nucleus. At $\mu = m_N - B_\alpha$ the BEC occurs in the ideal gas. Using Eq. (A1) one obtains the nucleon density in the BEC region

$$n_N = n_N^*(T) \simeq \frac{g_N}{\lambda_N^3(T)} \Phi_{3/2}^+ \left(-\frac{B_\alpha}{T} \right), \quad (8)$$

where $\Phi_{3/2}^+(\eta)$ is a dimensionless function defined in Appendix. Note that n_N^* does not depend on n_{bc} . From Eqs. (7) and (8), one can get the following relations for the ideal $\alpha - N$ gas in the BEC domain

$$\frac{n_N}{n_\alpha} \leq \frac{n_N^*}{n_\alpha^*} < \frac{1}{2\zeta(3/2)} e^{-B_\alpha/T}. \quad (9)$$

Here we take into account that $\Phi_{3/2}^+(\eta) < e^\eta$ and $\lambda_\alpha/\lambda_N \simeq 1/2$. According to (9), the fraction of unbound nucleons is small in the whole BEC region, especially at low temperatures (this conclusion has been earlier made in Ref. [24]). Figure 1 shows n_α^*, n_N^* as well as the baryon density of the ideal gas at the BEC boundary as functions of T . One can see that $n_N^* \ll n_\alpha^*$ even at large temperatures.

At each temperature, the chemical equilibrium condition (1) gives a line of allowable states in the (n_N, n_α) plane. These lines are shown in Fig. 2. Vertical sections of the lines correspond to the BEC states with densities $n_N = n_N^*(T)$ and $n_\alpha > n_\alpha^*(T)$. Such states lie above the BEC boundary shown by the thin solid curve in Fig. 2.

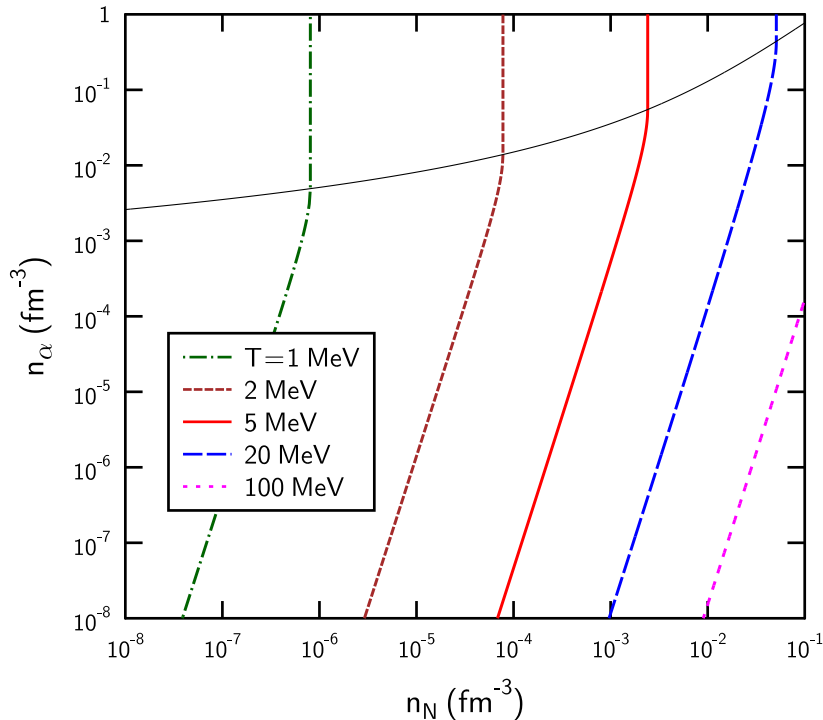


FIG. 2: Isotherms of chemical equilibrium for ideal $\alpha - N$ gas. The thin solid line shows boundary of BEC region.

C. Pure nucleon matter

Let us consider the limiting case of the one-component, iso-symmetric nucleon matter with interaction. The EoS and the phase diagram of a pure N -matter were studied by many authors. In particular, the mean-field approximation has been applied in Refs. [25–27]. In such an approach, one introduces a shift of the chemical potential μ_N with respect to the ideal nucleon gas. We apply the equation

$$\tilde{\mu}_N = \mu_N - U_N(n_N), \quad (10)$$

where $U_N(n_N)$ is the mean-field potential of nucleons and $\tilde{\mu}_N = \tilde{\mu}_N(T, n_N)$ is the effective chemical potential of nucleons at the density n_N and temperature T . This quantity is determined by solving Eq. (5) with $i = N$ and $\mu_i = \tilde{\mu}_N$. Here and below we neglect a possible explicit dependence of the mean-field potential on temperature. Equation (10) leads to the expression

$$\Delta p_N \equiv p_N(T, \mu_N) - p_N^{\text{id}}(T, \tilde{\mu}_N) = n_N U_N(n_N) - \int_0^{n_N} dn_1 U_N(n_1) \quad (11)$$

for the shift of the nucleon pressure with respect to its ideal gas value¹. One can see that Δp_N does not depend on T . From Eqs. (10) and (11) one can prove validity of the thermodynamic consistency relation, $n_N = (\partial p_N / \partial \mu_N)_T$.

Further on we use the Skyrme-like parametrization [27] of the mean field

$$U_N(n_N) = -2a_N n_N + \frac{\gamma + 2}{\gamma + 1} b_N n_N^{\gamma+1}, \quad (12)$$

where positive constants a_N, b_N, γ are adjustable parameters. The first and second terms describe, respectively, contributions of medium-range attractive and short-range repulsive interactions of nucleons. Substituting (12) into Eq. (11) one obtains

$$\Delta p_N = -a_N n_N^2 + b_N n_N^{\gamma+2}. \quad (13)$$

Parameters entering Eqs. (12) and (13) are chosen to reproduce phenomenological properties of equilibrium iso-symmetric nuclear matter at $T = 0$. We use the values [27]

$$\min \left(\frac{E}{B} \right) = -15.9 \text{ MeV}, \quad n_N = n_0 = 0.15 \text{ fm}^{-3} \quad (T = 0) \quad (14)$$

¹ This shift is often called as the 'excess' pressure [25, 26].

for the binding energy per baryon, $E/B = \varepsilon_N/n_N - m_N$, and the saturation density n_0 . Using further the thermodynamic identities at zero temperature, $p_N = n_N^2 d(\varepsilon_N/n_N)/dn_N$ and $\mu_N = (\varepsilon_N + p_N)/n_N$, one finds the equations which are equivalent to (14):

$$\mu_N = \mu_0 = 923 \text{ MeV}, \quad p_N = 0 \quad (T = 0, n_N = n_0). \quad (15)$$

At $T \rightarrow 0$ one can calculate the integrals in Eqs. (4) and (5) for $i = N$ analytically. In this limit the Fermi distributions inside these integrals can be replaced by unity if $k < k_F$ where $k_F = (6\pi^2 n_N/g_N)^{1/3}$ is the Fermi momentum of nucleons. One gets the relations

$$\tilde{\mu}_N(T = 0, n_N) = E_F(n_N) = \sqrt{k_F^2 + m_N^2}, \quad p_N^{\text{id}}(T = 0, n_N) = \frac{g_N}{6\pi^2} \int_0^{k_F} \frac{k^4 dk}{\sqrt{k^2 + m_N^2}}. \quad (16)$$

From Eqs. (10)–(11) and (15)–(16) one obtains two equations

$$U_N(n_0) = \mu_0 - E_F(n_0), \quad \Delta p_N(n_0) = -p_N^{\text{id}}(T = 0, n_0) \quad (17)$$

for the parameters a_N, b_N as functions of γ .

The results of numerical calculation for $\gamma = 1/6$ and $\gamma = 1$ are shown in Table I. In addition to coefficients of the Skyrme interactions, we also present the values of the incompressibility modulus

$$K_N = 9 \frac{dp_N}{dn_N} = 9n_N \frac{d(E_F + U_N)}{dn_N} \quad (18)$$

at the saturation point $n_N = n_0$, $T = 0$. As noted in Ref. [28], the Skyrme-like models with $1/6 \leq \gamma \leq 1/3$ predict reasonable values of the nuclear matter compressibility $K_N = 200 - 240 \text{ MeV}^2$. This agrees with our calculations. Indeed, one can see from Table I that the 'soft' Skyrme parametrization with $\gamma = 1/6$ is preferable as compared to $\gamma = 1$.

TABLE I: Characteristics of pure nucleon matter in Skyrme mean-field model.

γ	a_N (GeV fm ³)	b_N (GeV fm ^{3+3γ)}	K_N (MeV)	T_c (MeV)	n_c (fm ⁻³)	$\mu_c - m_N$ (MeV)
1/6	1.167	1.475	198	15.3	0.048	-31.6
1	0.399	2.049	372	21.3	0.059	-42.8

² See, however, Ref. [29] where higher values, $K_N = 250 - 315 \text{ MeV}$, have been obtained from the fit of data on the giant monopole resonance.

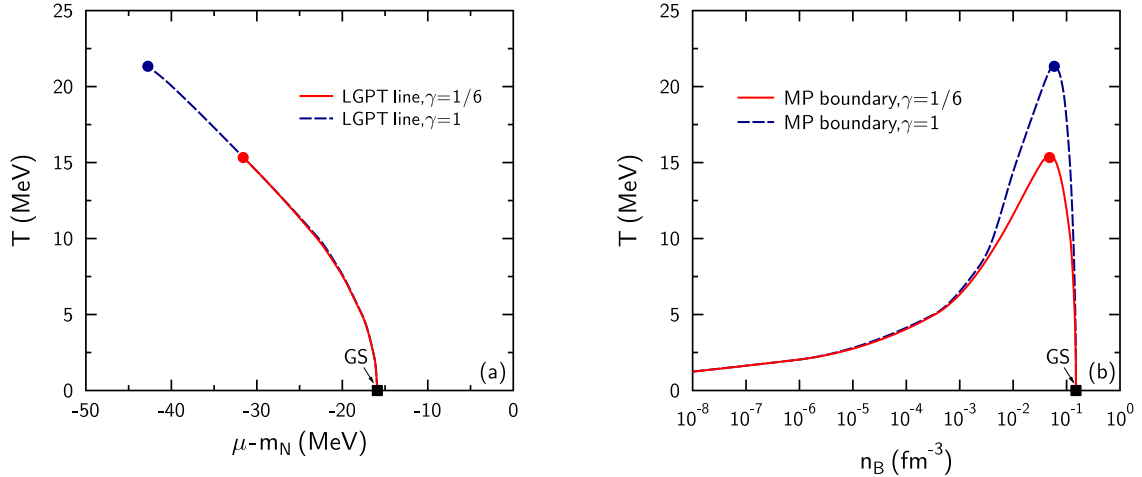


FIG. 3: Phase diagrams of iso-symmetric nucleon matter in (μ, T) (a) and (n_B, T) (b) planes. The solid and dashed lines correspond to LGPT at $\gamma = 1/6$ and $\gamma = 1$, respectively. Full dots mark positions of critical points. The ground state is shown by the full square.

Using Eqs. (2), (4)–(5), and (10)–(13) one can calculate all thermodynamic functions of a pure nucleon matter at nonzero temperatures. Our mean-field model predicts a first-order LGPT at temperatures $0 \leq T \leq T_c$, where T_c is the critical temperature. Characteristics of the LGPT are found by using the Gibbs conditions of the phase equilibrium [30]. For isotherms with $T < T_c$ there are two (meta)stable branches of the chemical potential as the function of pressure. In accordance with the Gibbs rule, these branches intersect at the LGPT point. We find the intersection points numerically by calculating isotherms in the chemical potential–pressure plane. Position of the critical point is found by solving two equations [30]: $(\partial p_N / \partial n_N)_T = 0$, $(\partial^2 p_N / \partial^2 n_N)_T = 0$. Characteristics of this point for the soft ($\gamma = 1/6$) and stiff ($\gamma = 1$) repulsive interaction are given in the last three columns of Table I.

Figures 3(a) and (b) show the phase diagrams of nucleonic matter in the (μ, T) and (n_B, T) planes, respectively. The LGPT line in Fig. 3(a) goes from the ground state (GS) at $T = 0$, $\mu = \mu_0$ to the critical point at $T = T_c$, $\mu = \mu_c$. According to our calculations, T_c increases, but μ_c decreases with γ . Figure 3(b) shows the ‘binodals’, i.e., the boundaries of the liquid-gas mixed phase (MP). They intersect the density axis at $n_B = n_N = n_0$.

D. Pure alpha matter

In this section we consider the idealized case of a pure alpha matter. In this limit reactions $\alpha \leftrightarrow 4N$ are disregarded and, therefore, the chemical equilibrium is violated. Up to now the EoS of such matter is poorly known. The variational microscopic calculations based on phenomenological $\alpha\alpha$ potentials were made a long time ago in Ref. [7]. More recently the EoS of a pure α matter was considered within several simplified models in Refs. [10, 11]. In Ref. [6] the phase diagram of such matter has been studied within a Skyrme mean-field model. Below we apply the same approach and use characteristics of the α -matter GS obtained in Ref. [7]:

$$W_\alpha = -\min\left(\frac{E_\alpha}{B}\right) = 12 \text{ MeV}, \quad n_\alpha = n_{0\alpha} = 0.036 \text{ fm}^{-3} \quad (T = 0). \quad (19)$$

Note that the baryon density of this state, $4n_{0\alpha} \simeq 0.144 \text{ fm}^{-3}$, is close to the saturation density of a pure nucleon matter, but the latter has stronger binding per baryon (compare Eqs. (14) and (19)).

In the case of a pure α matter, one can write the equations, analogous to Eqs. (10)–(13)

$$\tilde{\mu}_\alpha = 4\mu - U_\alpha(n_\alpha), \quad p_\alpha = p_\alpha^{\text{id}}(T, \tilde{\mu}_\alpha) + \Delta p_\alpha(n_\alpha), \quad (20)$$

where μ is the baryon chemical potential, and U_α and Δp_α are parameterized by Eqs. (12) and (13) with the replacement $N \rightarrow \alpha$. Below we choose the same parameter γ as for nucleons and find the coefficients a_α and b_α from the conditions (19).

In our mean-field model, one has the following relations for states with the BEC of alpha particles

$$\tilde{\mu}_\alpha = m_\alpha, \quad n_\alpha \geq n_\alpha^*(T), \quad p_\alpha^{\text{id}} = p_\alpha^*(T), \quad (21)$$

where n_α^* and p_α^* are defined in Eq. (7). The boundary of the BEC region is obtained after replacing the inequality in (21) by the equality. Solving the resulting equation, $4\mu = m_\alpha + U_\alpha[n_\alpha^*(T)]$, gives a line in the (μ, T) plane. For brevity, we call it as the BEC line.

At zero temperature $n_\alpha^* = 0$ and $p_\alpha^* = 0$ and the conditions (21) hold for all states. In this case Eqs. (20) give

$$4\mu = m_\alpha + U_\alpha(n_\alpha), \quad p_\alpha = \Delta p_\alpha(n_\alpha) \quad (T = 0). \quad (22)$$

Using further the relations $E_\alpha/B = \varepsilon_\alpha/4n_\alpha - m_N$ and $p_\alpha = 4\mu n_\alpha - \varepsilon_\alpha = 0$ for the GS of alpha matter, one gets algebraic equations for coefficients of the Skyrme interaction [6]:

$$U_\alpha(n_{0\alpha}) = 4(B_\alpha - W_\alpha), \quad \Delta p_\alpha(n_{0\alpha}) = 0, \quad (23)$$

where B_α was introduced in Sec. II B. The solutions of Eqs. (23) can be written as

$$a_\alpha = b_\alpha n_{0\alpha}^\gamma = \frac{4(\gamma + 1)}{\gamma n_{0\alpha}} (W_\alpha - B_\alpha). \quad (24)$$

Numerical values of the coefficients a_α and b_α as well as the compressibility $K_\alpha = 9\gamma a_\alpha n_{0\alpha}$ are given in Table II for the soft and stiff Skyrme repulsion.

TABLE II: Characteristics of pure alpha matter in Skyrme model.

γ	a_α (GeV fm ³)	b_α (GeV fm ^{3+3γ)}	K_α (MeV)	T_c (MeV)	n_{Bc} (fm ⁻³)	$\mu_c - m_N$ (MeV)	T_{tp} (MeV)
1/6	3.831	6.667	207	10.2	0.037	-16.7	3.56
1	1.094	30.39	354	13.7	0.048	-19.3	3.65

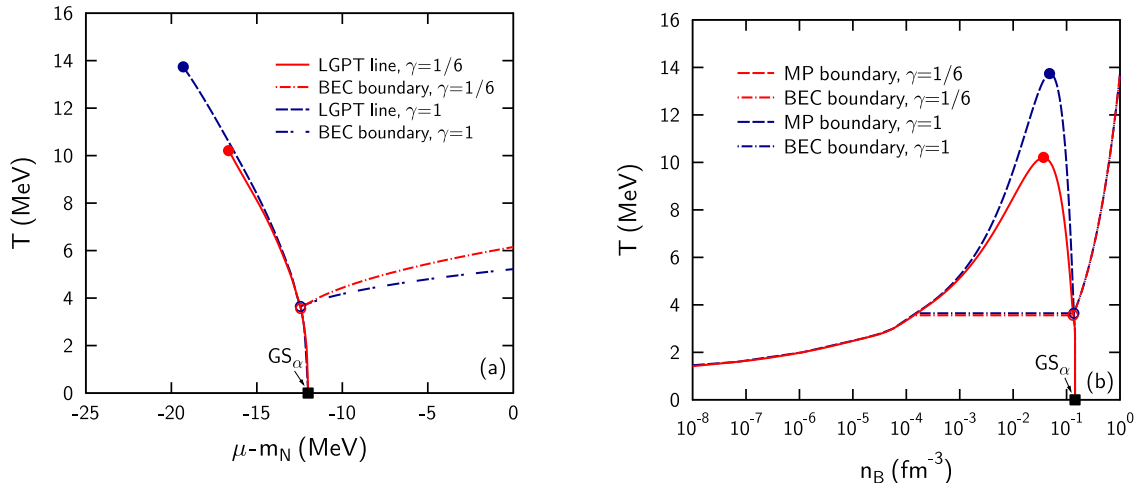


FIG. 4: Phase diagrams of pure alpha matter in (μ, T) (a) and (n_B, T) (b) planes. The solid and dashed curves correspond to $\gamma = 1/6$ and $\gamma = 1$, respectively. Full dots mark positions of critical points. The GS of alpha matter is shown by the full square. The dash-dotted lines represent boundaries of BEC regions. Open dots show positions of triple points. They practically coincide for two considered values of γ .

Using the Skyrme interaction one can calculate the thermodynamical functions of a pure alpha matter at nonzero temperatures. Similarly to the pure nucleon matter, the model

predicts the LGPT in a pure alpha system. In the (μ, T) plane this phase transition occurs along a line which goes from the GS at $T = 0$ to the critical point at $T = T_c, \mu = \mu_c$. A presence of the BEC imposes some complications as compared to the case of a pure nucleon matter. We found that the BEC boundary crosses the LGPT line at some 'triple' point with temperature $T_{\text{tp}} < T_c$.

The resulting phase diagrams in the (μ, T) and (n_B, T) planes are shown in Figs. 4(a) and (b), respectively (note that $n_B = 4n_\alpha$ for a pure α matter). Characteristics of the critical point as well as the temperature of the triple point are given in Table II. Similar to a pure nucleon matter, the value of T_c (μ_c) increases (decreases) with γ , but the position of the triple point only slightly depends on this parameter. Note that the BEC region in Fig. 4(a) extends to the right from the LGPT line and below the BEC line. According to Fig. 4(b), the BEC line in the (n_B, T) plane is not sensitive to γ outside the MP region. It is clear that inside this region the BEC occurs only in the liquid phase, which volume fraction diminishes with decreasing n_B . Therefore, the volume fraction of the condensate decreases too and vanishes on the left binodal boundary. The horizontal lines in Fig. 4(b) show the BEC critical temperatures in the MP domain for two considered values of γ .

III. SKYRME MODEL FOR $\alpha - N$ BINARY MIXTURE

A. Thermodynamic relations for two-component system

Similarly to one-component matter, we take into account multiparticle interactions in the $\alpha - N$ mixture by introducing a temperature-independent excess part of pressure Δp

$$p = p_N^{\text{id}}(T, n_N) + p_\alpha^{\text{id}}(T, n_\alpha) + \Delta p(n_N, n_\alpha). \quad (25)$$

A similar expression can be written for the free energy density, $f = \sum_{i=N,\alpha} \mu_i n_i - p$, after introducing the excess term $\Delta f = f - f_N^{\text{id}} - f_\alpha^{\text{id}}$. At known Δp one can calculate the mean-field potentials $U_i = \mu_i - \tilde{\mu}_i$ as well as the excess free energy Δf . The following relations can be obtained [31, 32]

$$U_N(n_N, n_\alpha) = \left(\frac{\partial \Delta f}{\partial n_N} \right)_{n_\alpha}, \quad U_\alpha(n_N, n_\alpha) = \left(\frac{\partial \Delta f}{\partial n_\alpha} \right)_{n_N}, \quad \Delta f(n_N, n_\alpha) = \int_0^1 \frac{d\lambda}{\lambda^2} \Delta p(\lambda n_N, \lambda n_\alpha). \quad (26)$$

In addition, one can find the entropy density $s = -\partial f/\partial T = \sum_i s_i^{\text{id}}$ and the energy density $\varepsilon = f + Ts = \sum_i \varepsilon_i^{\text{id}} + \Delta f$, where s_i^{id} and $\varepsilon_i^{\text{id}}$ are the corresponding ideal-gas quantities for i th species ($i = N, \alpha$).

The free energy density is a genuine thermodynamic potential in the canonical ensemble. Instead of partial densities n_N and n_α one can also use the variables

$$n_B = n_N + 4n_\alpha, \quad \chi = \frac{4n_\alpha}{n_B}. \quad (27)$$

The quantity χ is a fraction of bound nucleons in the $\alpha - N$ matter (it is approximately equal to the mass fraction of alphas). Note that due to the baryon number conservation, $B = N_N + 4N_\alpha = \text{const}$, the baryon density n_B is inversely proportional to the system volume V . Using Eq. (27) and thermodynamic identities, one can write the following relations for changes of the free energy per baryon in any isothermal process

$$d\left(\frac{F}{B}\right) = d\left(\frac{f}{n_B}\right) = p \frac{dn_B}{n_B^2} + \left(\frac{\mu_\alpha}{4} - \mu_N\right) d\chi \quad (T = \text{const}). \quad (28)$$

According to this equation, at fixed T and n_B the quantity F/B reaches its extremum if the condition (1) is satisfied. However, solving Eq. (1) with respect to χ does not necessarily gives the true state of chemical equilibrium. In particular, the solution can be unstable ($F/B = \text{max}$) if the second derivative of F/B over χ is negative.

In general, one should explicitly calculate the curvature matrix $(\partial^2 f/\partial n_i \partial n_j)_T$ to study stability of the system with respect to fluctuations of partial densities n_N, n_α . Only if both eigenvalues of this matrix are nonnegative, the corresponding state will be stable³. The necessary condition of stability can be written as [33]

$$\det\left(\frac{\partial^2 f}{\partial n_i \partial n_j}\right)_T = \det\left(\frac{\partial \mu_i}{\partial n_j}\right)_T = \left(\frac{\partial \mu_N}{\partial n_N}\right)_T \left(\frac{\partial \mu_\alpha}{\partial n_\alpha}\right)_T - \left(\frac{\partial \mu_N}{\partial n_\alpha}\right)_T^2 \geq 0. \quad (29)$$

B. Skyrme parametrization of interaction terms

In the present paper we apply a generalized Skyrme-like parametrization for the excess pressure Δp :

$$\Delta p(n_N, n_\alpha) = - \sum_{i,j} a_{ij} n_i n_j + \left(\sum_i B_i n_i \right)^{\gamma+2}, \quad (30)$$

³ Note, that appearance of negative-curvature (spinodal) parts of the free-energy density surface can be considered as a necessary condition for the LGPT.

where a_{ij} , B_i , and γ are positive constants and the sums go over $i, j = N, \alpha$. The first term in the right hand side of Eq. (30) describes attractive forces and has the same structure as in the two-component van der Waals equation of state [16]. The second term, responsible for repulsive interactions, is obtained by interpolation between the limits $n_\alpha = 0$ and $n_N = 0$ considered in Sec. II C and II D. From the comparison with these limiting cases one gets the relations $a_{ii} = a_i, B_i^{\gamma+2} = b_i$ where a_i and b_i are the Skyrme coefficients introduced earlier for the pure nucleon ($i = N$) and pure alpha ($i = \alpha$) matter. Using these relations, one finds

$$\Delta p(n_N, n_\alpha) = -(a_N n_N^2 + 2a_{N\alpha} n_N n_\alpha + a_\alpha n_\alpha^2) + b_N (n_N + \xi n_\alpha)^{\gamma+2}, \quad (31)$$

where

$$\xi = \left(\frac{b_\alpha}{b_N} \right)^{1/(\gamma+2)} = \begin{cases} 2.006, & \gamma = 1/6, \\ 2.457, & \gamma = 1. \end{cases} \quad (32)$$

Numerical values of ξ in Eq. (32) are obtained by substituting the b_N and b_α values from Tables I and II. One can see that there is only one unknown coefficient in the parametrization (31), namely the cross-term coefficient $a_{N\alpha}$ which determines the $\alpha - N$ attraction strength. Below we study the sensitivity to the choice of this parameter.

Using Eqs. (26) and (31) one gets the relations

$$\Delta f = -(a_N n_N^2 + 2a_{N\alpha} n_N n_\alpha + a_\alpha n_\alpha^2) + \frac{b_N}{\gamma+1} (n_N + \xi n_\alpha)^{\gamma+2}, \quad (33)$$

$$\mu_N = \tilde{\mu}_N - 2(a_N n_N + a_{N\alpha} n_\alpha) + \frac{\gamma+2}{\gamma+1} b_N (n_N + \xi n_\alpha)^{\gamma+1}, \quad (34)$$

$$\mu_\alpha = \tilde{\mu}_\alpha - 2(a_{N\alpha} n_N + a_\alpha n_\alpha) + \frac{\gamma+2}{\gamma+1} b_N \xi (n_N + \xi n_\alpha)^{\gamma+1}. \quad (35)$$

To study the EoS of interacting $\alpha - N$ matter we choose a certain value of $a_{N\alpha}$ and substitute (34) and (35) into the condition of chemical equilibrium (1). The resulting equation gives allowable states in the (T, n_N, n_α) space. Then from Eqs. (25), (31), and (34) we determine pressure at different $\mu = \mu_N$ and T .

Before going to numerical results we would like to note that our approach becomes questionable at high densities of α particles. Classical Monte-Carlo calculations in the hard-sphere approximation show [34] that the transition to a ‘solid’ phase occurs in a pure alpha system at $n_\alpha \gtrsim (0.07 - 0.1) \text{ fm}^{-3}$ (in this estimate we assume the radius of the α nucleus $r_\alpha = 1 - 1.2 \text{ fm}$). Therefore, our results should be considered with caution at baryon densities $n_B \gtrsim 0.3 - 0.4 \text{ fm}^{-3}$.

IV. RESULTS FOR INTERACTING $\alpha - N$ MATTER

A. Zero temperature limit

Let us consider first the ground state of the $\alpha - N$ matter at zero temperature. Note that this is the state with $p = 0$ and minimal energy per baryon ε/n_B . Using formulae of the preceding section one can calculate the pressure p , the baryon chemical potential

$$\mu = \mu_N = \mu_\alpha/4, \quad (36)$$

and the energy per baryon $\varepsilon/n_B = \mu - p/n_B$ at $T \rightarrow 0$ as functions of n_B for different values of the parameter $a_{N\alpha}$.

Our analysis shows that the results are qualitatively different if this parameter is smaller or larger than some threshold value a_* (see below Eq. (41)). In the region $a_{N\alpha} < a_*$ the GS of the $\alpha - N$ mixture corresponds to a pure nucleon matter ($n_\alpha = 0$) with $\mu = \mu_0$ and $n_N = n_0$. Here μ_0 and n_0 are, respectively, the chemical potential and the saturation density of the equilibrium nucleon matter, introduced in Sec. II C. In the same interval of $a_{N\alpha}$, there exists another local minimum of energy per baryon with $n_N = 0$ which corresponds to a pure alpha matter. This state is metastable because it has a smaller binding energy as compared to a pure nucleon matter. These two minima in the (n_B, χ) plane are separated by an energetic barrier.

Our calculations show that at $a_{N\alpha} > a_*$ the $\alpha - N$ mixture has only one minimum-energy state in the (n_B, χ) plane and this system becomes stronger bound as compared to a pure nucleon matter. In this region the GS is characterized by a nonzero value of n_α and the corresponding binding energy $W = m_N - \varepsilon/n_B = m_N - \mu$ increases with $a_{N\alpha}$.

The threshold value a_* can be found analytically by using formulae of preceding section. One should take into account that at zero temperature all α 's are Bose-condensed ($\tilde{\mu}_\alpha = m_\alpha$) and the ideal gas pressure $p_\alpha^{\text{id}} = 0$. Using these relations and formulas of Sec. III one gets the equations

$$p = p_N^{\text{id}} + \Delta p(n_N, n_\alpha) = 0, \quad (37)$$

$$\mu_N = E_F(n_N) + U_N(n_N, n_\alpha), \quad (38)$$

$$\mu_\alpha = m_\alpha + U_\alpha(n_N, n_\alpha), \quad (39)$$

where $\Delta p, U_N, U_\alpha$ are functions of n_N, n_α defined in Eqs. (31), (34)–(35).

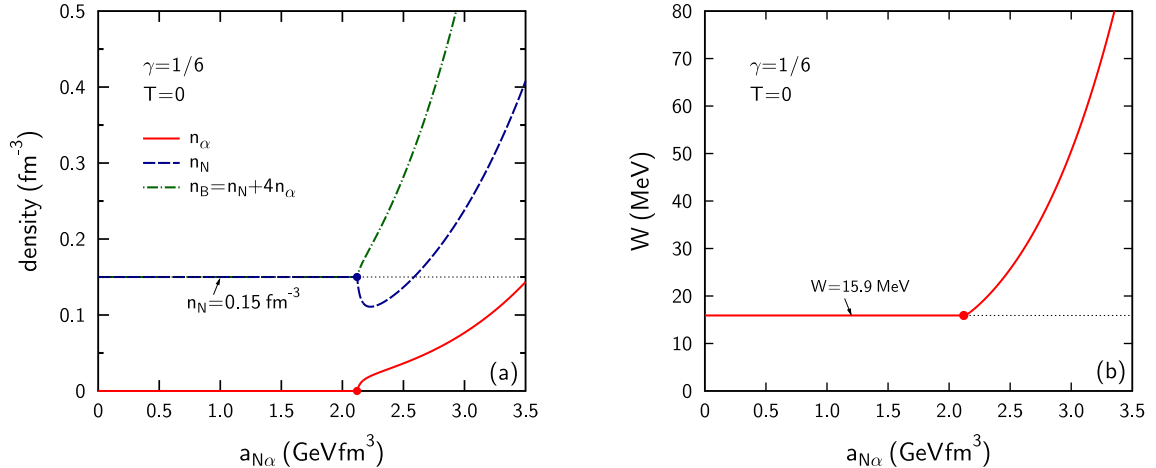


FIG. 5: (a) Partial densities as well as baryon density of particles in GS of cold $\alpha - N$ matter as functions of cross-term coefficient $a_{N\alpha}$. (b) Binding energy per baryon of cold $\alpha - N$ mixture as the function of $a_{N\alpha}$. Dots correspond to threshold value $a_{N\alpha} = a_*$ (see text). All calculations correspond to $\gamma = 1/6$.

The ground-state values of μ, n_B, χ are determined by simultaneously solving Eqs. (36)–(39). They are continuous functions of $a_{N\alpha}$, so that $\mu \rightarrow \mu_0, n_N \rightarrow n_0, n_\alpha \rightarrow 0$ at $a_{N\alpha} \rightarrow a_*$. Substituting these limiting values into (36), (39) gives

$$m_\alpha + U_\alpha(n_0, 0) = 4\mu_0 \quad (a_{N\alpha} = a_*). \quad (40)$$

Solving this equation with respect to a_* gives

$$a_* = \frac{1}{2} \left(\frac{m_\alpha - 4\mu_0}{n_0} + \frac{\gamma + 2}{\gamma + 1} b_N \xi n_0^\gamma \right) \simeq 2.12 \text{ GeVfm}^3 \quad (\gamma = 1/6). \quad (41)$$

In the last equality we use numerical values of b_N, ξ obtained in Sec. II C and III B.

Figures 5(a) and (b) show ground-state characteristics of a cold $\alpha - N$ matter as functions of $a_{N\alpha}$ for $\gamma = 1/6$. One can see that at $a_{N\alpha} > a_*$ the binding energy and densities n_α, n_B increase monotonically with $a_{N\alpha}$.

Below we present the results for $\gamma = 1/6$ and choose the parameter $a_{N\alpha}$ in the interval $a_{N\alpha} < a_*$, i.e., assume that alphas do not appear in the GS at $T \rightarrow 0$. Such an assumption seems to be supported by the nuclear phenomenology. To study the sensitivity to $a_{N\alpha}$, we compare the results for $a_{N\alpha} = 1$ (set A) and 1.9 (set B) GeVfm^3 .

B. Phase diagram of interacting $\alpha - N$ matter

In this section we consider the EoS of the chemically equilibrated $\alpha - N$ mixture at nonzero temperatures. We apply explicit relations for pressure and free energy derived in Sec. III B. By solving Eq. (1) one can find allowable states of matter in the (T, μ, p) or (T, n_N, n_α) space. Stability of such states is studied by calculating the sign of the determinant in Eq. (29).

Figure 6 represents the isotherm $T = 2$ MeV in the plane (μ, p) . Lower and upper panels correspond to sets A and B, respectively. Unstable parts of the isotherm are shown by dotted lines. It is interesting that only these parts exhibit significant changes in the transition between sets A and B. According to the Gibbs rule, intersection points of (meta)stable branches of pressure as functions of μ correspond to phase transitions (PT). As one can see from Fig. 6, there are two PT at $T = 2$ MeV. Their characteristics, in particular, critical values of the baryon chemical potential μ_c are given in Table III.

The first transition, PT_1 , occurs at a smaller baryon chemical potential as compared to PT_2 ⁴. As a consequence, states on the dashed lines have smaller pressure (i.e. larger thermodynamic potential $\Omega = -pV$) as compared to states with the same μ on the solid curve. It is well-known, that states with smaller pressure are thermodynamically less favorable [30, 35]. This shows that states on dashed lines (including mixed-phase states of PT_2) are metastable. In Figs. 6–8 stable (favorable) states are represented by the solid lines and metastable (unfavorable) states are indicated by the dashed lines. The unstable states with maximum values of Ω are shown by dotted lines.

Figures 7(a) and (b) represent the same isotherm $T = 2$ MeV, but in the (n_N, n_α) plane. A strong sensitivity to $a_{N\alpha}$ is clearly visible in this representation. By shading we show the region of BEC $n_\alpha > n_\alpha^* \simeq 0.014 \text{ fm}^{-3}$ (see Sec. II B). For both sets of parameters we do not find any stable states of the $\alpha - N$ matter with large fraction of alphas at densities $n_N \gtrsim 10^{-2} \text{ fm}^{-3}$. One may say that the model imitates the Mott effect [36], i.e., predicts a suppression of nuclear clusters at large baryon densities. On the other hand, the model predicts metastable states, where α particles are more abundant than nucleons (see, e.g., upper parts of Figs. 7, 8 where the dashed lines enter the shaded area).

⁴ Note that the slope of pressure as a function of μ equals the baryon density n_B . Therefore, jumps of the pressure slopes at points PT_1 and PT_2 in Fig. 6, correspond to nonzero jumps of n_B .

TABLE III: Characteristics of LGPT for $\alpha - N$ matter at $T = 2$ MeV (set B).

	binodal point C					binodal point D			
	$\mu_c - m_N$ (MeV)	n_N (fm $^{-3}$)	n_α (fm $^{-3}$)	n_B (fm $^{-3}$)	χ	n_N (fm $^{-3}$)	n_α (fm $^{-3}$)	n_B (fm $^{-3}$)	χ
PT $_1$	-16.2	$8.2 \cdot 10^{-7}$	$6.3 \cdot 10^{-11}$	$8.2 \cdot 10^{-7}$	$3.1 \cdot 10^{-4}$	0.15	$2.1 \cdot 10^{-17}$	0.15	$1.4 \cdot 10^{-16}$
PT $_2$	-12.1	$6.4 \cdot 10^{-6}$	$2.3 \cdot 10^{-7}$	$7.3 \cdot 10^{-6}$	0.12	$7.3 \cdot 10^{-4}$	$3.5 \cdot 10^{-2}$	0.14	1.0

Points C_i and D_i in Fig. 7 and Table III are the binodal points (i.e. boundaries of the liquid-gas MP) for the phase transition PT $_i$ ($i = 1, 2$). Coordinates of such points in the (n_N, n_α) plane are determined from the Gibbs conditions of phase equilibrium:

$$p\left(T, n_N^{(C)}, n_\alpha^{(C)}\right) = p\left(T, n_N^{(D)}, n_\alpha^{(D)}\right) = p_c, \quad (42)$$

$$\mu_N\left(T, n_N^{(C)}, n_\alpha^{(C)}\right) = \mu_N\left(T, n_N^{(D)}, n_\alpha^{(D)}\right) = \mu_c, \quad (43)$$

where we omit indices i . Characteristics of binodal points for the parameter set B are given in Table III⁵. We have checked that at $T = 2$ MeV the nucleon densities at points C_1 and D_1 are close to binodal densities of a pure nucleon matter (see Sec. II C). The same conclusion is valid for the alpha-particle densities at points C_2 and D_2 : they are close to the binodal densities obtained for a pure alpha matter in Sec. II D. Note that for both parameter sets point D_2 lies in the BEC region.

The solid and short-dashed lines C_1D_1 and C_2D_2 in Fig. 7 correspond to the MP states for PT $_1$ and PT $_2$, respectively. Coordinates of these states in the (n_N, n_α) plane and the volume fraction of the liquid phase, λ , satisfy the relations (as above, we omit the phase transition index)

$$\lambda = \frac{n_N - n_N^{(C)}}{n_N^{(D)} - n_N^{(C)}} = \frac{n_\alpha - n_\alpha^{(C)}}{n_\alpha^{(D)} - n_\alpha^{(C)}}. \quad (44)$$

One can see that the MP states lie on the straight lines in the (n_N, n_α) plane. However, one can hardly recognize this linear dependence in Fig. 7 because of the double-logarithmic scale used in this plot.

As one can see from Table III and Fig. 7, the mass fraction of alphas, χ , is relatively small for the MP states of PT $_1$, but it is rather large for the transition PT $_2$. As has been

⁵ Calculation with set A gives a very small value (about 10^{-74} fm $^{-3}$) for the alpha-particle density at the binodal point D_1 . The latter lies far below the horizontal axis in Fig. 7(a).

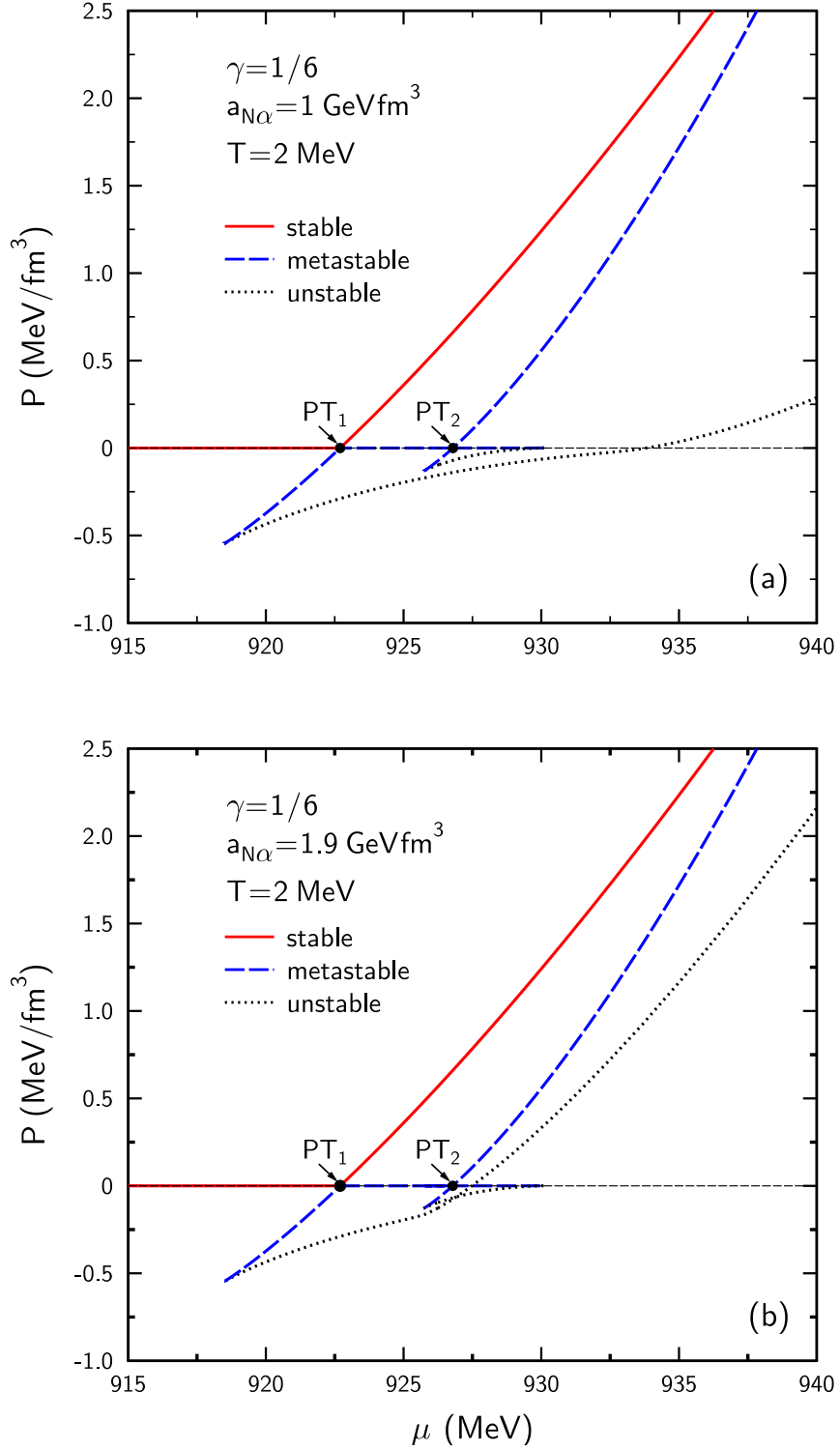


FIG. 6: The isotherm $T = 2$ MeV of $\alpha - N$ matter in (μ, p) plane for the parameter sets A (a) and B (b). The stable, metastable and unstable parts of isotherm are shown by the solid, dashed and dotted lines, respectively. The dots PT_1 and PT_2 show positions of stable and metastable LGPT, respectively.

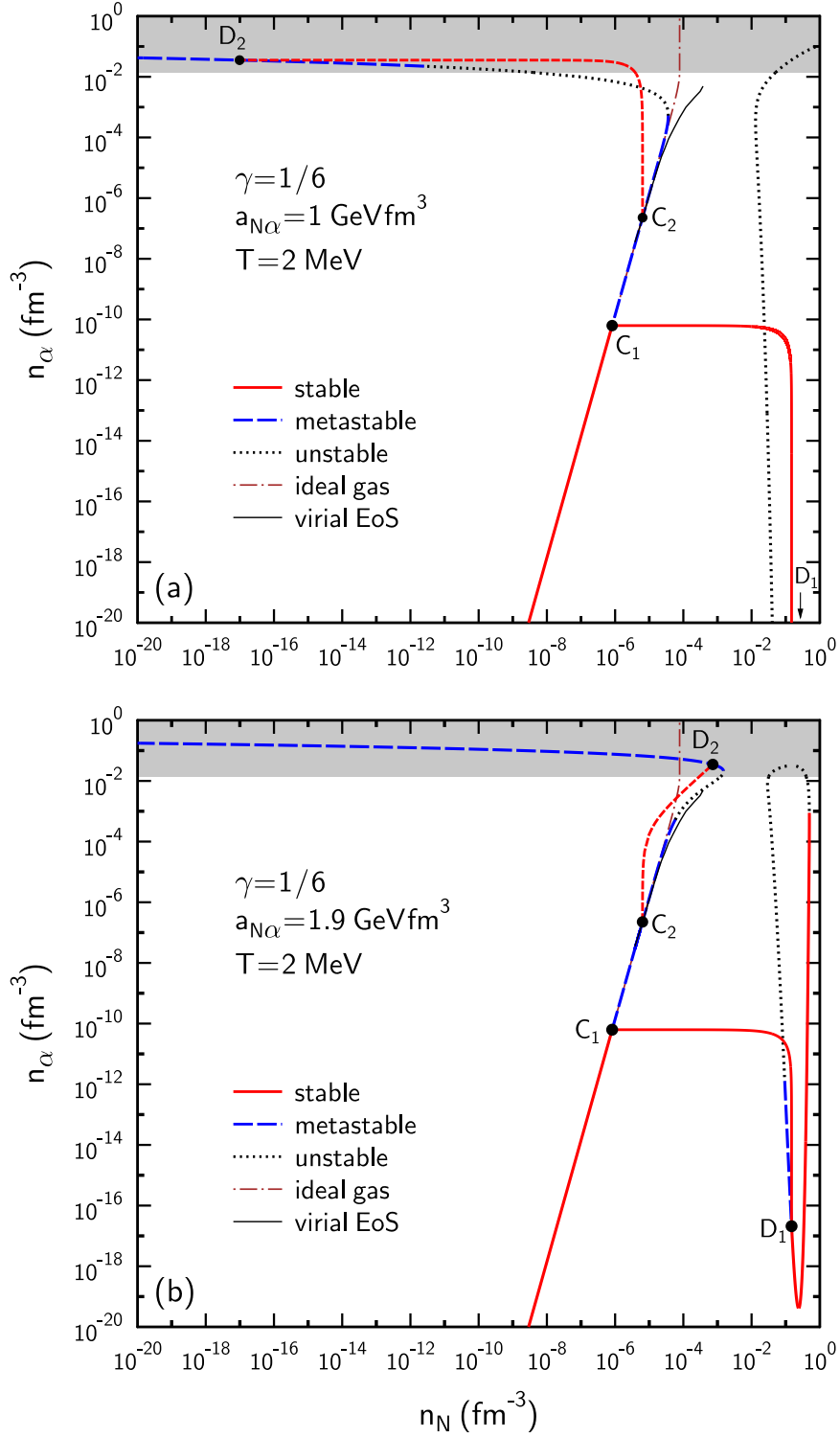


FIG. 7: The isotherm $T = 2$ MeV in (n_N, n_α) plane for the same parameters as in Fig. 6. The BEC region is shown by shading. The dash-dotted line corresponds to ideal $\alpha - N$ gas. Lines C_1D_1 and C_2D_2 correspond to mixed-phase states of PT_1 and PT_2 , respectively. The thin solid line represents the isotherm $T = 2$ MeV from Ref. [15]. Note that binodal point D_1 in upper panel lies below the plotted region.

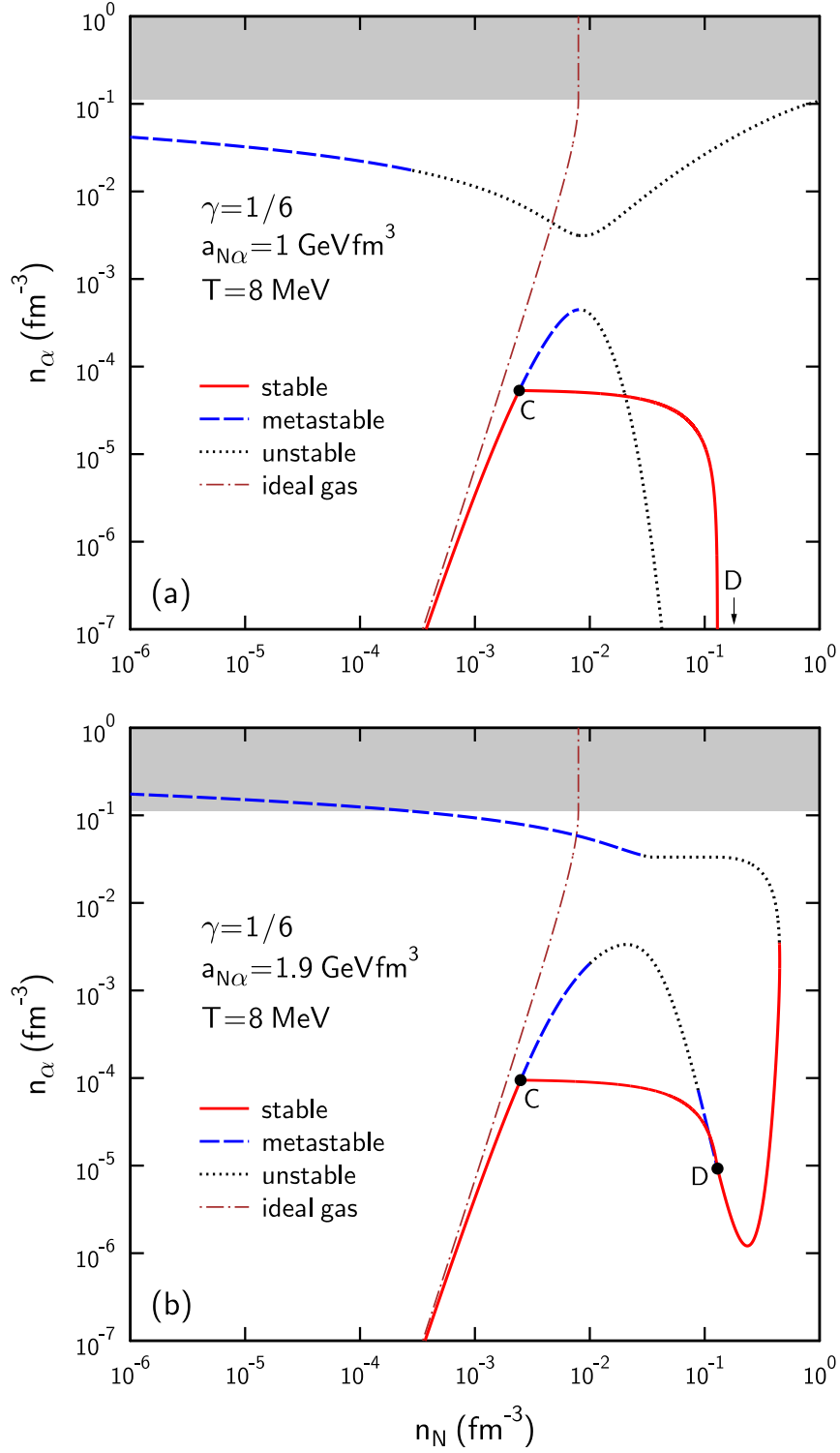


FIG. 8: Same as Fig. 7 but for $T = 8$ MeV. Note that only one (stable) LGPT exists at this temperature.

already mentioned, the phase transition PT_2 is in fact metastable. Nevertheless, we believe

that it can be observed in dynamical processes (like heavy-ion collisions) by selecting states with large relative abundances of α 's. The same statement can be made for BEC states (see the dashed lines in the shaded regions). Indications of enhanced production of so-called α -conjugate nuclei have been observed recently in intermediate-energy nuclear collisions [37].

The results obtained within a virial approach [15] are shown in Fig. 7 by thin solid lines. This approximation can be considered as reasonable only at low densities. Note that the quantum-statistical and phase transition effects are disregarded in such a model. Nevertheless, from Fig. 7 one can conclude that calculations with set B are in better agreement with the results of Ref. [15]. Presumably, this parameter set is preferable as compared to set A.

Figures 8(a) and (b) show the isotherm $T = 8$ MeV in the (n_N, n_α) plane, again for the parameter sets A and B. At this temperature only one, stable LGPT remains. One can see a significant change in shape of the isotherm as compared to the case $T = 2$ MeV considered in Fig. 7.

TABLE IV: Characteristics of phase transitions in $\alpha - N$ matter for parameter sets A and B.

	PT ₁				PT ₂				
	T_{CP} (MeV)	$\mu_{\text{CP}} - m_N$ (MeV)	n_{BCP} (fm ⁻³)	χ_{CP}	T_K (MeV)	$\mu_K - m_N$ (MeV)	n_{BK} (fm ⁻³)	χ_K	T_{TP} (MeV)
set A	15.4	-31.7	$4.8 \cdot 10^{-2}$	$2.5 \cdot 10^{-4}$	7.6	-14.3	$(1.2 - 2.6) \cdot 10^{-2}$	0.14 - 1.0	3.54
set B	14.7	-30.3	$5.3 \cdot 10^{-2}$	$6.9 \cdot 10^{-2}$	4.6	-13.2	$1.3 \cdot 10^{-3} - 10^{-1}$	0.46 - 0.86	3.37

Further increase of T leads to disappearance of the LGPT. This takes place at $T > T_{\text{CP}}$ where T_{CP} is the temperature of the critical point. Similar to pure nucleon and alpha matter, we determine characteristics of this point by simultaneously solving the equations $(\partial p / \partial n_B)_T = 0$ and $(\partial^2 p / \partial^2 n_B)_T = 0$. Our analysis shows that the metastable transition PT₂ disappears 'abruptly' at some temperature, T_K which is smaller than T_{CP} . Note that there is still a nonzero baryon density jump at $T = T_K$ (see Fig. 9(d))⁶.

⁶ This means that at $T > T_K$ there are no additional intersections between the pressure branches in the (μ, p) plane except the point PT₁. We found, that pressure slopes on both sides of the point PT₂ still differ when $T \rightarrow T_K$. On the other hand, the density jump disappears for the transition PT₁ when $T \rightarrow T_{\text{CP}}$.

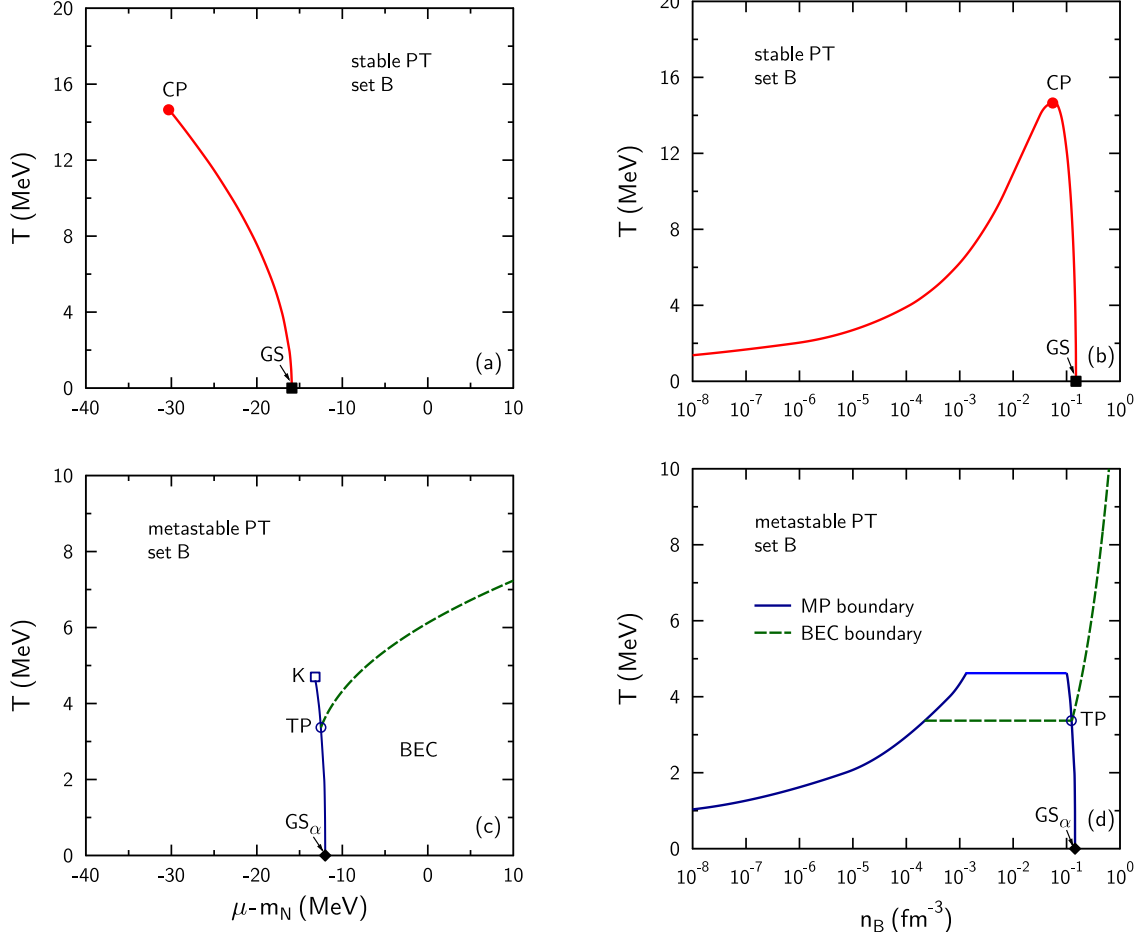


FIG. 9: Left panels: critical lines of stable (a) and metastable (c) PT of $\alpha - N$ matter in (μ, T) plane. Right panels: boundaries of MP for stable (b) and metastable (d) PT of $\alpha - N$ mixture in (n_B, T) plane. All calculations correspond to parameter set B. Full circles in (a) and (b) show positions of critical point. The dashed lines in (c) and (d) represent boundaries of BEC region. The open square (circle) marks the end (triple) point of the metastable PT. Full squares and diamonds show, respectively, the GS positions for pure nucleon and pure alpha matter.

Table IV gives characteristics of the critical point of the PT_1 as well as those for the end point K of the PT_2 . One can see that position of the critical point CP is not very sensitive to the parameter $a_{N\alpha}$. On the other hand, characteristics of PT_2 are stronger modified in the transition between sets A and B.

A more detailed information is given in Figs. 9(a)–(d) which represent the phase diagrams of the $\alpha - N$ matter in the (μ, T) and (n_B, T) planes. Qualitatively, the critical line of the metastable PT in the (μ, T) plane is similar to that for a pure α matter (see Fig. 4(a)).

Note however, that the end point K can not be regarded as a critical point. The full square and diamonds in Figs. 9 mark, respectively, the ground states of one-component systems composed of nucleons or alphas. These states coincide with boundaries of critical lines on the axis $T = 0$.

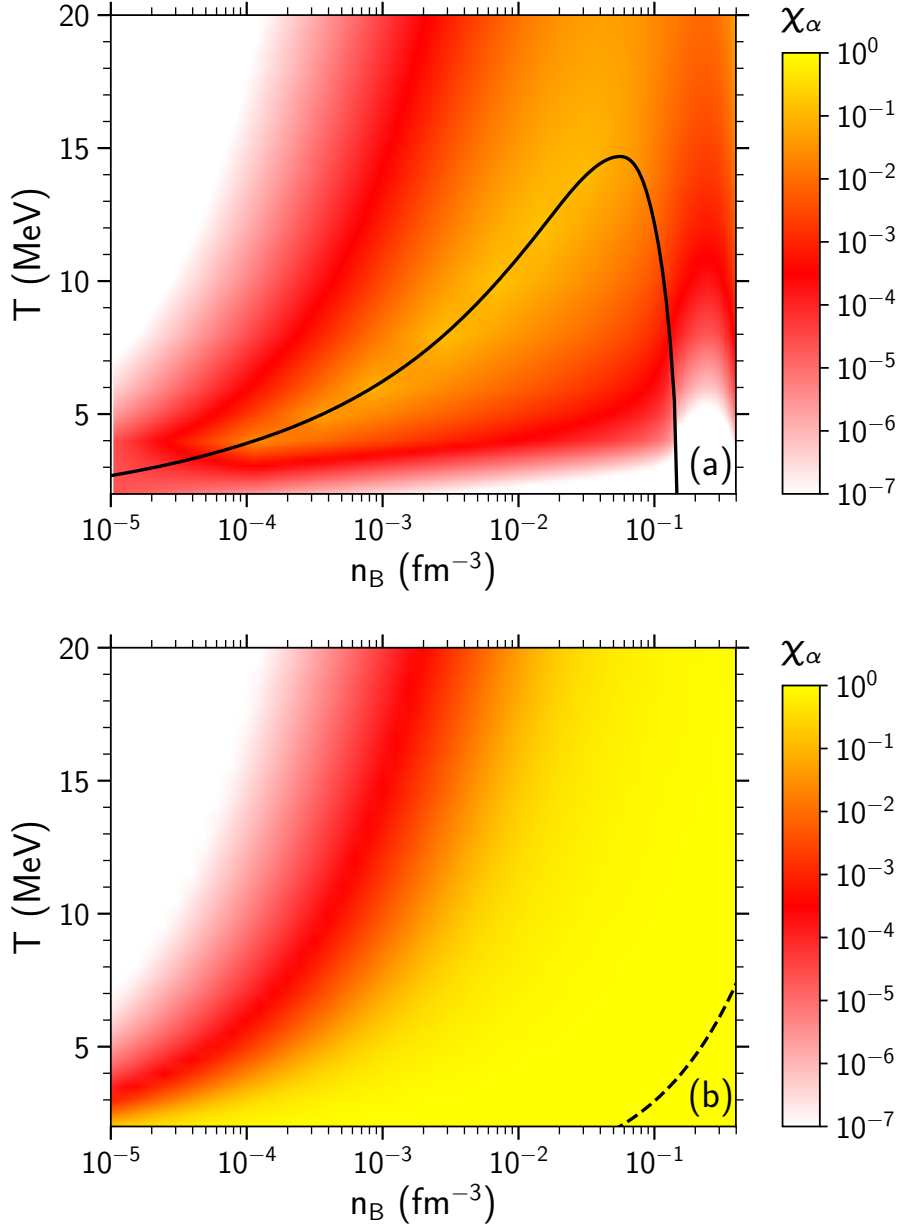


FIG. 10: (a) Contour plot of the mass fraction of α 's in $\alpha - N$ matter for parameter set B. The MP boundary is shown by the solid line. (b) Same as in upper panel, but for ideal $\alpha - N$ gas. The dashed line represents the BEC boundary.

The contour plot of the mass fraction χ in the (n_B, T) plane is shown in Fig. 10(a) for the parameter set B. In this calculation we take into account only stable states of the $\alpha - N$ matter. One can see that maximum values $\chi \sim 0.1 - 0.2$ are reached near the left boundary of LGPT⁷. At fixed temperature χ decreases with n_B in the MP region. It is interesting that similar nonmonotonic density behavior of χ was also predicted in Refs. [2, 16, 20, 21, 23]. We would like to emphasize that the model gives qualitatively different results as compared to the ideal $\alpha - N$ gas where the mass fraction of α 's increases monotonically with n_B (see Fig. 10(b)).

V. CONCLUSIONS AND OUTLOOK

In this paper we have analyzed the EoS and phase diagram of the chemically equilibrated $\alpha - N$ matter. Our approach simultaneously takes into account the quantum-statistical effects as well as liquid-gas phase transitions. We apply Skyrme-like parametrizations of interaction terms as functions of particle densities. The model parameters were chosen by using the ground-state characteristics of a pure nucleon and pure alpha matter at zero temperature. We investigate stability of the $\alpha - N$ mixture with respect to density fluctuations. The regions of possible phase transitions have been studied for different choices of model parameters. At low enough temperatures two LGPT are found, where one is stable and other is metastable. It is demonstrated that the phase transition effects are important even for dilute states of the $\alpha - N$ matter. A strong suppression of alpha-cluster abundance is found at large nucleon densities. On the other hand, nucleon fractions are relatively small for metastable states with Bose-Einstein condensation of alphas.

The results of this paper may be used for studying nuclear cluster production in heavy-ion reaction as well as in astrophysics. To analyze dynamical processes in nuclear collisions, it would be interesting to calculate not only isotherms but also trajectories of constant entropy per baryon. Then one can study a possibility to reach the metastable states of α condensation in the course of isentropic expansion of excited matter produced in a heavy-ion collision.

In the present paper we use parametrizations of mean-fields which predict two separated

⁷ Note that much larger relative abundances of α 's and even their BEC can be reached by selecting metastable states of the $\alpha - N$ matter.

minima of the energy per baryon of cold $\alpha - N$ matter. These minima correspond to the ground states of pure nucleon and pure α matter. Another possibility, where the nuclear matter has only one ground state composed of nucleons with a small admixture of α 's, will be considered in the subsequent paper.

In the future, we are going to apply our approach for studies of clusterized isospin-asymmetric matter as expected in compact stars and their merges. More realistic calculations can be made by taking into account the Coulomb interactions as well as contributions of other light and heavy clusters. The results of this paper may be useful for investigating not only equilibrium, but also nonequilibrium mixtures of nucleons and nuclear clusters. We think that the present model can be also used to study properties of binary mixtures of fermionic atoms and bosonic molecules, like $H + H_2$ or $D + D_2$.

Acknowledgments

I.N.M. acknowledges the financial support of the Helmholtz International Center for FAIR research. The work of M.I.G. is supported by the Alexander von Humboldt Foundation and by the Goal-oriented Program of National the Academy of Sciences of Ukraine. L.M.S. thanks for the support from the Frankfurt Institute for Advanced Studies. H.St. appreciates the support from J. M. Eisenberg Laureatus chair.

Appendix A: Thermodynamic functions of ideal nucleon and alpha gas

Let us consider the case $\mu_\alpha < m_\alpha$ when the density of Bose-condensed alphas $n_{bc} = 0$. In the lowest order in T/m_i ($i = N, \alpha$) one gets from Eqs. (4), (5) the relations [38]

$$n_i \simeq \frac{g_i}{\lambda_i^3(T)} \Phi_{3/2}^\pm \left(\frac{\mu_i - m_i}{T} \right), \quad p_i^{\text{id}} \simeq \frac{g_i T}{\lambda_i^3(T)} \Phi_{5/2}^\pm \left(\frac{\mu_i - m_i}{T} \right) \quad (T \ll m_i). \quad (\text{A1})$$

Here upper and lower signs correspond to $i = N$ and $i = \alpha$, respectively, $\lambda_i(T)$ is the thermal wave length introduced in Sec. II B, and

$$\Phi_\beta^\pm(\eta) \equiv \frac{1}{\Gamma(\beta)} \int_0^\infty \frac{x^{\beta-1} dx}{e^{x-\eta} \pm 1}, \quad (\text{A2})$$

where $\Gamma(\beta)$ is the gamma function⁸. For $\eta \leq 0$ one can use the decomposition in powers of fugacity: $\Phi_{\beta}^{\pm}(\eta) = \sum_{k=1}^{\infty} (\mp 1)^{(k+1)} k^{-\beta} \exp(\eta k)$. At $\eta = 0$ functions (A2) are expressed through the Riemann zeta function $\zeta(\beta)$:

$$\Phi_{\beta}^{-}(0) = \zeta(\beta), \quad \Phi_{\beta}^{+}(0) = (1 - 2^{1-\beta}) \zeta(\beta). \quad (\text{A3})$$

The classical Boltzmann approximation corresponds to the limit $\mu_i - m_i \rightarrow -\infty$. Using the approximate relation $\Phi_{\beta}^{\pm}(\eta) \simeq e^{\eta}$ at $\eta \rightarrow -\infty$ one gets, instead of Eq. (A1), much simpler relations

$$n_i \simeq \frac{g_i}{\lambda_i^3(T)} \exp\left(\frac{\mu_i - m_i}{T}\right), \quad p_i^{\text{id}} \simeq n_i T \quad (n_i \lambda_i^3 \ll g_i). \quad (\text{A4})$$

-
- [1] J. P. Bondorf, *J. Phys. Colloq.* **37**, C5-195 (1976);
 J. P. Bondorf, A. S. Botvina, A. S. Illjinov, I. N. Mishustin, K. Sneppen,
Phys. Rep. **257**, 133 (1995).
- [2] J. M. Lattimer, F. D. Swesty, *Nucl. Phys. A* **535**, 331 (1991).
- [3] H. Stöcker, G. Buchwald, G. Graebner, P. Subramanian, J. A. Maruhn, W. Greiner,
 B. V. Jacak, G. D. Westfall, *Nucl. Phys. A* **400**, 63c (1983).
- [4] J. P. Bondorf, R. Donangelo, I. N. Mishustin, C. Pethick, H. Schultz, and K. Sneppen,
Nucl. Phys. A **443**, 321 (1985).
- [5] G. Peilert, J. Randrup, H. Stöcker and W. Greiner, *Phys. Lett. B* **260**, 271 (1991).
- [6] L. M. Satarov, M. I. Gorenstein, A. Motornenko, V. Vovchenko, I. N. Mishustin, H. Stoecker,
J. Phys. G **44**, 125102 (2017).
- [7] J. W. Clark, T.-P. Wang, *Ann. Phys.* **40**, 127 (1966).
- [8] M. T. Johnston, J. W. Clark, *Kinam* **2**, 3 (1980).
- [9] D. M. Brink, J. J. Castro, *Nucl. Phys. A* **216**, 109 (1973).
- [10] A. Sedrakian, H. Mütter, P. Schuck, *Nucl. Phys. A* **766**, 97 (2006).
- [11] Ş. Mişicu, I. N. Mishustin, W. Greiner, *Mod. Phys. Lett. A* **32**, 1750010 (2017).
- [12] H. Horiuchi, K. Ikeda, Y. Suzuki, *Suppl. Prog. Theor. Phys.* **52**, 89 (1972).

⁸ Note that $\Phi_{\beta}^{\pm}(\eta) = \mp Li_{\beta}(\mp e^{\eta})$ where $Li_{\beta}(x) = \sum_{k=1}^{\infty} x^k k^{-\beta}$ is the polylogarithm of the β -th order.

- [13] I. N. Mishustin, Phys. Scripta 80, 293 (1984).
- [14] A. Tohsaki, N. Itagaki, arXiv.org: 1809.00460.
- [15] C. J. Horowitz, A. Schwenk, Nucl. Phys. A **776**, 55 (2006).
- [16] V. Vovchenko, A. Motornenko, P. Alba, M. I. Gorenstein, L. M. Satarov, and H. Stoecker, Phys. Rev. C **96**, 045202 (2017).
- [17] A. S. Botvina and I. N. Mishustin, Nucl. Phys. A **843**, 98 (2010).
- [18] N. Buyukcizmeci *et al.*, Nucl. Phys. A **907**, 13 (2013).
- [19] S. Furusawa, I. Mishustin, Phys. Rev. C **97**, 025804 (2018).
- [20] M. Hempel, J. Schaffner-Bielich, Nucl. Phys. A **837**, 210 (2010).
- [21] H. Pais, F. Gulminelli, C. Providencia, G. Roepke, Phys. Rev. C **97**, 045805 (2018).
- [22] S. Typel, J. Phys. G **45**, 114001 (2018).
- [23] S. Lalit, M. A. A. Mamun, L. Constantinou, M. Prakash, arXiv: 1809.08126.
- [24] X.-H. Wu, S.-B. Wang, A. Sedrakian, G. Röpke, J. Low Temp. Phys. **189**, 133 (2017).
- [25] D. Anchishkin, Sov. Phys. JETP **75**, 195 (1992).
- [26] D. Anchishkin, E. Suhonen, Nucl. Phys. A **586**, 734 (1994).
- [27] L. M. Satarov, M. N. Dmitriev, I. N. Mishustin, Phys. At. Nucl. **72**, 1390 (2009).
- [28] M. Bender, P.-H. Heenen, P.-G. Reinhard, Rev. Mod. Phys. **75**, 121 (2003).
- [29] J. R. Stone, N. J. Stone, S. A. Moszkowski, Phys. Rev. C **89**, 044316 (2014).
- [30] L. D. Landau and E. M. Lifshitz, *Statistical Physics* (Pergamon, Oxford, 1975).
- [31] L. M. Satarov, K. A. Bugaev, I. N. Mishustin, Phys. Rev. C **91**, 055203 (2015).
- [32] L. M. Satarov, V. Vovchenko, P. Alba, M. I. Gorenstein, and H. Stoecker, Phys. Rev. C **95**, 024902 (2017).
- [33] H. Müller and B. D. Serot, Phys. Rev. C **52**, 2072 (1995).
- [34] *Theory and Simulation of Hard Sphere Fluids and Related Systems*, Lect. Notes Phys. Vol. 753, edited by A. Mulero (Springer, Berlin, 2008).
- [35] W. Greiner, L. Neise, and H. Stöcker, *Thermodynamics and Statistical Mechanics*, (Springer, Berlin, 1997).
- [36] G. Röpke, L. Münchov, H. Schulz, Nucl. Phys. A **379**, 536 (1982).
- [37] K. Schmidt *et al.*, Phys. Rev. C **95**, 054618 (2017).
- [38] Yu. M. Poluektov, A. A. Soroka, arXiv: 1709.09698.